Materials Research Proceedings **27** (2023) 207-214 https://doi.org/10.21741/9781644902455-26

Inverse finite element-based shape reconstruction method for large-scale space antenna

Tianxiang Huang[1, a*], Tianyu Dong[2, b] and Shenfang Yuan[2, c]

[1]College of Civil Aviation, Nanjing University of Aeronautics and Astronautics, Jiangjun Avenue 29, Nanjing 211106, China

[2]Research Center of Structural Health Monitoring and Prognosis, the State Key Laboratory of Mechanics and Control of Mechanical Structures, Nanjing University of Aeronautics and Astronautics, 29 Yudao Street, Nanjing 210016, China

[a]tianxiang.huang@nuaa.edu.cn, [b]dongty@nuaa.edu.cn, [c]ysf@nuaa.edu.cn

Keywords: Large Scale Space Antenna, Thermal Deformation, Shape Reconstruction, Inverse Finite Element, Element Optimization

Abstract. Large-scale space antennas will experience rapid temperature changes and non-uniform temperature distribution during orbit operation. These thermal excitations will lead to unpredictable deformation of the antenna. To ensure its normal operation, real-time and reliable shape monitoring of the antenna is necessary for further array correction and compensation. The structural shape reconstruction method based on strain information and fiber Bragg grating sensors is one of the most potent methods. This paper proposed an inverse finite element-based shape reconstruction method with variable element size for a honeycomb sandwich antenna panel under changing and non-uniform temperature environment. The size of the inverse finite element is optimized by the displacement gradient, which reduces the total number of elements and improves the efficiency of the shape reconstruction algorithm. The proposed method is validated with a honeycomb sandwich antenna panel numerically and experimentally.

Introduction

In the field of communication, reconnaissance, remote sensing, and deep space exploration, large-scale space antennas have been widely used and play a decisive role in the function of the satellite system [1]. During orbit operation, space antennas will experience rapid temperature changes due to solar radiation and non-uniform temperature distribution due to functional devices [2]. These thermal excitations will lead to unpredictable deformation of the antenna.

To ensure the operation of space antennas, real-time and reliable shape monitoring of the antenna is necessary for further array correction and compensation. The shape reconstruction method based on strain information and fiber Bragg grating sensors is one of the most potent methods as it can achieve real-time monitoring and the weight of the monitoring system is more lightweight than other methods [3].

The key to the strain-based shape sensing method is to accurately establish the relationship between strain and displacement. A lot of methods have been proposed, such as Ko's displacement theory [4], modal transformation theory [5], curvature-based method [6], and inverse finite element method (iFEM) [7]. Among them, the iFEM method is independent of the loading conditions and material information of the structure, which can be considered a promising candidate for the shape sensing of space antennas.

For the large-scale space antennas, the iFEM method needs a large number of elements for shape reconstruction, which will not meet the real-time reconstruction requirement of the shape reconstruction algorithm. The efficiency of the iFEM-based shape reconstruction method is related to the number of elements in the method [8]. Thus, an optimized element discretization method is needed to increase the efficiency of the iFEM method while the accuracy can be maintained.

Thus, this paper proposes an element discretization method based on the displacement gradient for the iFEM shape reconstruction method. By optimizing the size of the inverse element, the number of elements for the iFEM method can be highly reduced, which can increase the efficiency of the shape reconstruction method while maintaining accuracy. The Basic principle of the variable-size inverse finite element method is first given. Then the numerical model of the space antenna is described. The displacement and strain distribution of the structure is analyzed. At last, the shape reconstruction results of the optimized element and original element are compared.

The variable-size inverse finite element method

Element discretization method based on displacement gradient

The first step of the iFEM method is to discretize the structure into a number of finite elements. Then the inverse finite element can be applied. The number of the inverse element has a great influence on the accuracy and speed of the reconstruction method. Thus, this paper proposed a displacement gradient-based-element discretization method to optimize the number of the inverse finite elements.

The proposed element discretization method will be conducted on the numerical model of the structure, as the numerical model of the structure can be acquired during the design and manufacturing process. From the numerical model, the displacement distribution of the structure can be acquired. For example, Fig. 1 shows the contour plot of the displacement distribution. A proper gradient of the displacement can be determined according to the accuracy requirements of the shape reconstruction and the amount of structural deformation. Then, based on the displacement gradient, the optimized size of the element in x-direction and y-direction can be determined as illustrated in Fig. 2. At last, the structure is discretized by the optimized elements.

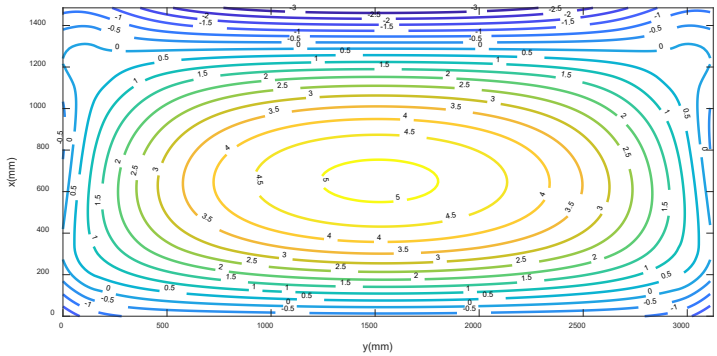

Fig. 1 The contour plot of the displacement distribution

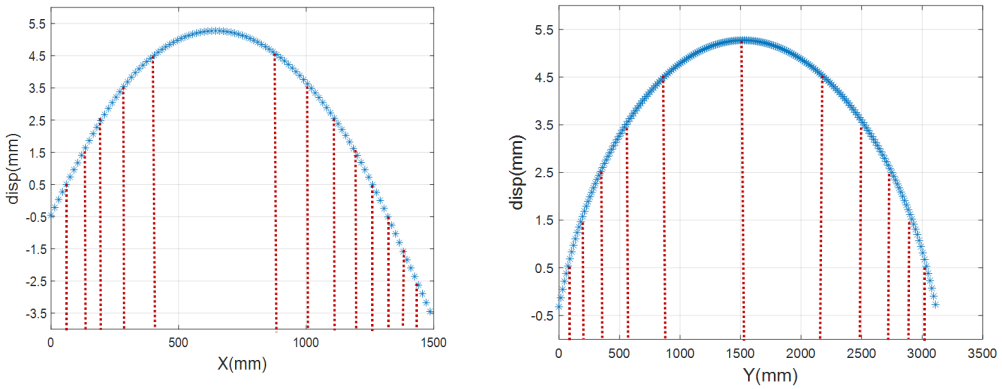

(a) x-direction (b) y-direction

Fig. 2 Optimized size of the element

Materials Research Proceedings **27** (2023) 207-214 https://doi.org/10.21741/9781644902455-26

The implementation process of the variable-size inverse finite element method

The element adopted in this paper is the four-node quadrilateral inverse-shell element (iQS4) as illustrated in Fig. 3. The displacement nodal vector of the element can be expressed as follows

$$\boldsymbol{u}^e = \begin{bmatrix} \boldsymbol{u}_1 & \boldsymbol{u}_2 & \boldsymbol{u}_3 & \boldsymbol{u}_4 \end{bmatrix}^T \tag{1}$$

where

$$\boldsymbol{u}_i = \begin{bmatrix} u_i & v_i & w_i & \theta_{xi} & \theta_{yi} & \theta_{zi} \end{bmatrix}^T, (i = 1,2,3,4). \tag{2}$$

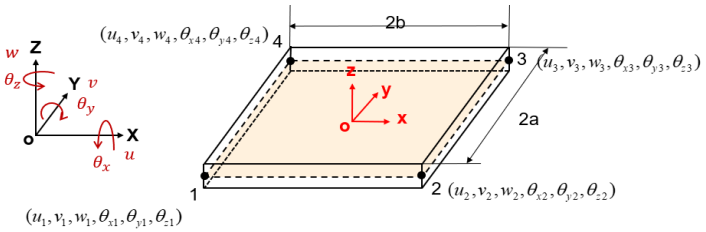

Fig. 3 Four-node quadrilateral inverse-shell element

The measured strain can be expressed in terms of the element nodal displacement vector as

$$\begin{Bmatrix} \varepsilon_x \\ \varepsilon_y \\ \gamma_{xy} \end{Bmatrix} = e(\boldsymbol{u}^e) + z\kappa(\boldsymbol{u}^e) = B_m \boldsymbol{u}^e + zB_\kappa \boldsymbol{u}^e$$
$$\begin{Bmatrix} \gamma_{xz} \\ \gamma_{yz} \end{Bmatrix} = g(\boldsymbol{u}^e) = B_s \boldsymbol{u}^e \tag{3}$$

where the matrices, B_m, B_κ and B_s, contain derivatives of the shape functions.

The strain sensors are arranged on the surface of the element as illustrated in Fig. 4. According to Eq. (3), the membrane section strain and the curvatures can be expressed as the measured strain as follows

$$e = \frac{1}{2}\left(\begin{Bmatrix} \varepsilon_x \\ \varepsilon_y \\ \gamma_x \end{Bmatrix}^+ + \begin{Bmatrix} \varepsilon_x \\ \varepsilon_y \\ \gamma_x \end{Bmatrix}^- \right)$$
$$\kappa = \frac{1}{H}\left(\begin{Bmatrix} \varepsilon_x \\ \varepsilon_y \\ \gamma_x \end{Bmatrix}^+ - \begin{Bmatrix} \varepsilon_x \\ \varepsilon_y \\ \gamma_x \end{Bmatrix}^- \right) \tag{4}$$

where the superscripts '+' and '-' denote the quantities that correspond to the top and bottom surface locations, respectively.

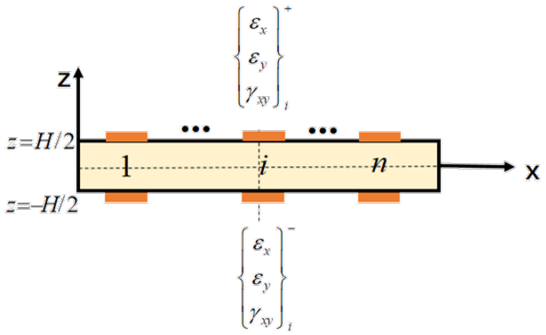

Fig. 4 The strain sensors arranged on the surface of the element

For each element, the functional accounted the deformation can be expressed as

$$\Phi_e(\boldsymbol{u}^e) = \left\| e(\boldsymbol{u}^e) - e^{\varepsilon} \right\|^2 + \left\| \kappa(\boldsymbol{u}^e) - \kappa^{\varepsilon} \right\|^2 + \lambda \left\| g(\boldsymbol{u}^e) - g^{\varepsilon} \right\|^2 \tag{5}$$

By minimizing the weighted least squares of the functional in Eq. (5) with respect to the nodal displacement $\boldsymbol{u}^e$

$$\frac{\partial \Phi_e(\boldsymbol{u}^e)}{\partial \boldsymbol{u}^e} = 0 \tag{6}$$

The displacement-strain relation in each element can be expressed as

$$\mathbf{k}^e \boldsymbol{a}^e = \mathbf{f}^e \tag{7}$$

where

$$\mathbf{k}^e = \int_A B_m{}^T B_m + H^2 B_\kappa{}^T B_\kappa + \lambda B_s{}^T B_s dA \tag{8}$$

$$\mathbf{f}^e = \frac{1}{n} \int_A \sum_{i=1}^{n} \left(B_m{}^T e_i^{\varepsilon} + \frac{H^2}{n} B_\kappa{}^T k_i^{\varepsilon} \right) dA \tag{9}$$

The global displacement-strain relation can be acquired by assembling the element displacement-strain relation according to the element nodal, which gives

$$\mathbf{KU} = \mathbf{F} \tag{10}$$

By including the boundary conditions, the global displacement-strain relation can be expressed in the reduced form. And the displacement of all elements can be acquired as

$$\mathbf{U}^R = (\mathbf{K}^R)^{-1} \mathbf{F}^R \tag{11}$$

Numerical study of the large-scale space antenna

Numerical Model

The dimension of the antenna is 1500mm×3125mm×20mm. It is a typical sandwich structure with epoxy fiberglass as the face sheet and aramid paper honeycomb as the core. Four aluminum blocks with a T shape are inserted in the honeycomb as illustrated in Fig. 5. The material properties are

listed in Table 1. The tails of the T-shaped aluminum block are clamped as the boundary condition. The temperature field applied to the structure is acquired from the experiment with thermocouple sensors, as shown in Fig. 6.

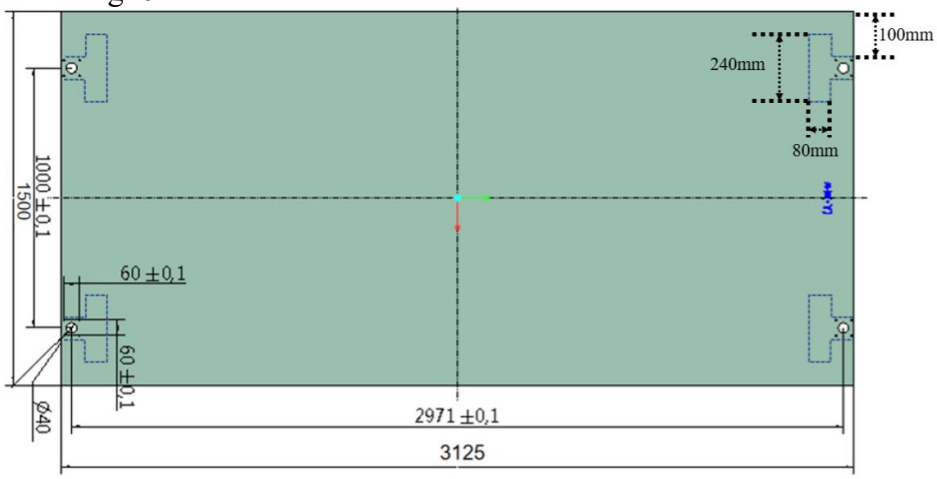

Fig. 5 The geometry of the antenna

Table 1 The material properties

	Aluminum	Honeycomb	Face sheet
Density （t/mm^3）	7.2E-09	7.2E-11	1.85E-09
Elastic modulus （MPa）	70000	E_1=0.1 E_2=0.1 E_3=0.1	E_1=24100 E_2=22400 E_3=0
Poisson's ratio	0.3	μ_{12}=0.3 μ_{13}=0 μ_{23}=0	μ_{12}=0.32 μ_{13}=0 μ_{23}=0
Shear modulus （MPa）	/	G_{12}=0.1 G_{13}=43.2 G_{23}=21.6	G_{12}=4300 G_{13}=1470 G_{23}=1470
Thermal expansion coefficient （°C^{-1}）	2.32E-05	α_{11}=1.23E-05 α_{22}=1.23E-05 α_{33}=0	α_{11}=1.23E-05 α_{22}=1.23E-05 α_{33}=0

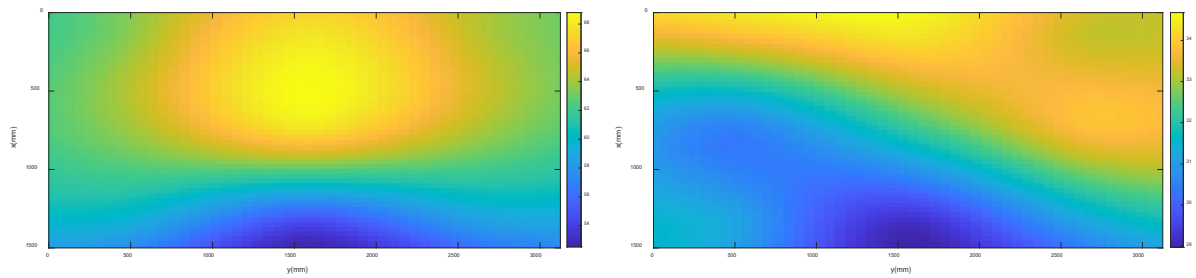

(a) Surface with heating device (b) Surface without heating device

Fig. 6 The measured temperature field

Numerical results

With the numerical model, the displacement and strain distribution can be acquired as illustrated in Fig. 7. The strain field on the optimized elements can be acquired as shown in Fig. 8.

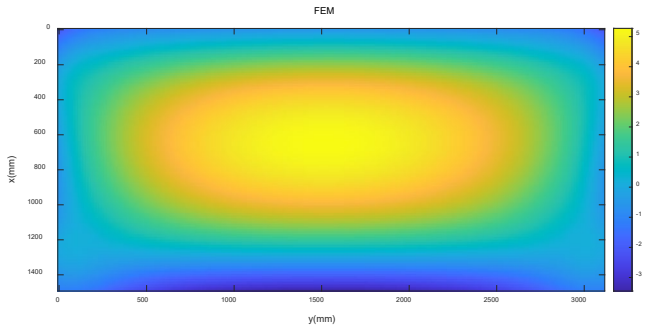

Fig. 7 Displacement distribution of the antenna

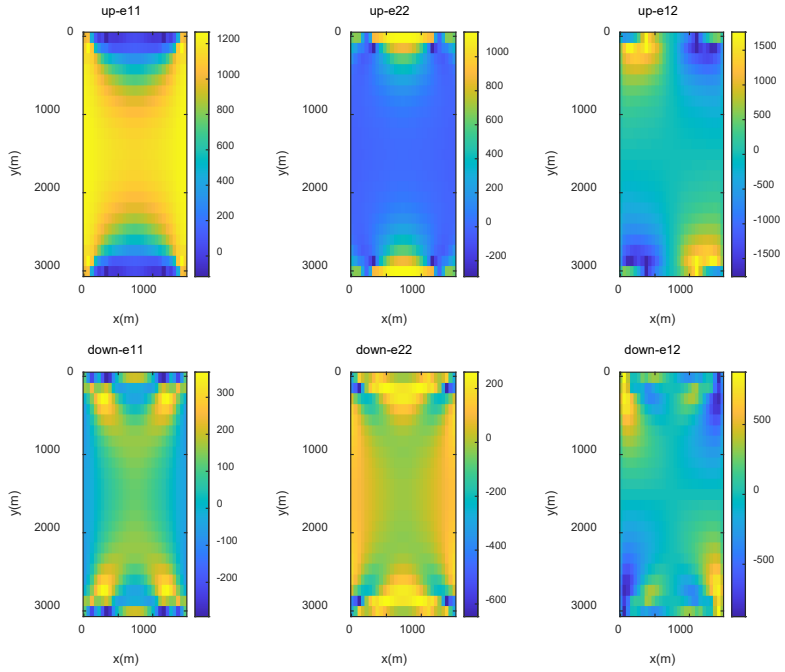

Fig. 8 Strain field of both surfaces

The shape reconstruction results

Based on the displacement field and accuracy requirement, the gradient of the displacement is set to be 1 mm. The optimized element size is determined with the element discretization method based on displacement gradient as illustrated in Fig. 9 (a) with a total number of 165 elements. while the original discretization needs 667element.

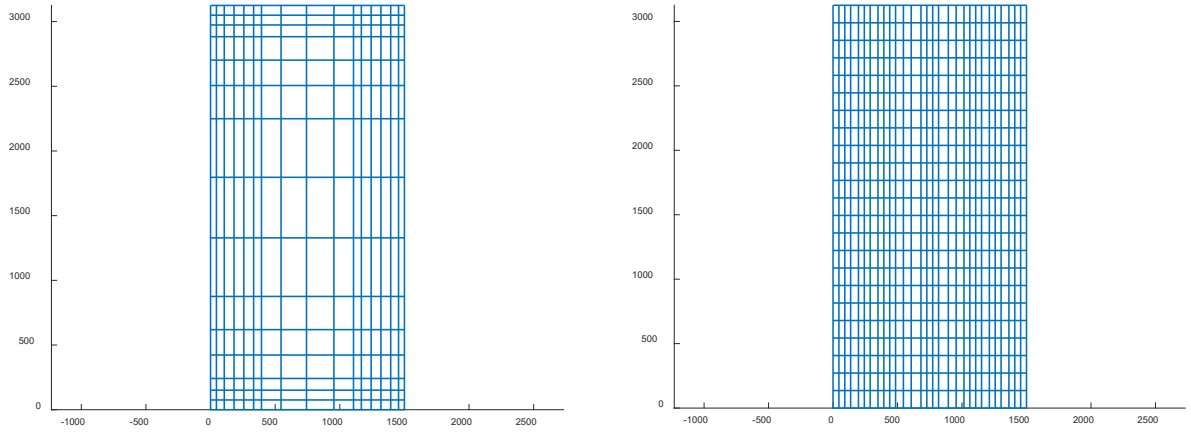

(a) Optimized (b) original

Fig. 9 Elements discretization cases (mm)

The shape reconstruction results with optimized and original element discretization are shown in Fig. 10 and Fig. 11. The error of the optimized elements is 0.83 mm, while the error of the original elements is 0.86 mm.

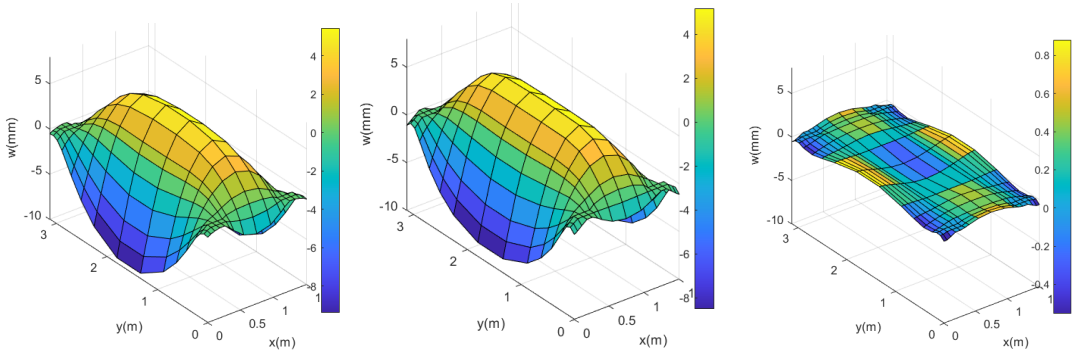

(a) Reconstructed displacement (b) FEM displacement (c) Error

Fig. 10 Shape reconstruction results with the optimized elements

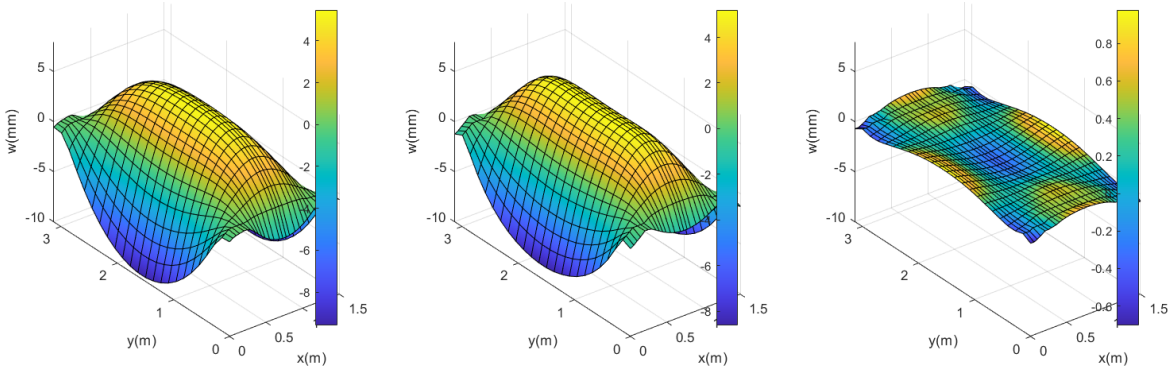

(a) Reconstructed displacement (b) FEM displacement (c) Error

Fig. 11 Shape reconstruction results with the original elements

Summary

In this paper, a variable-size inverse finite element method is proposed for the shape reconstruction of the large-scale space antenna structure under thermal excitation. The size of the inverse finite element is optimized by the displacement gradient, which reduces the total number of elements and improves the efficiency of the shape reconstruction algorithm. The numerical results show that the number of elements is reduced from 667 to 165. The proposed method is validated on the large-

scale space antenna structure under a non-uniform temperature field. The error of reconstructed displacement is less than 1 mm.

References

[1] William A. Imbriale, et al., Space Antenna Handbook, Wiley, 2012.

[2] Guang-Yu Lu, Ji-Yang Zhou and Guo-Ping Cai, et al., Studies of thermal deformation and shape control of a space planar phased array antenna, Aerospace Science and Technology, 2019, 93, 105311.

[3] Jason P. Moore and Matthew D. Rogge, Shape sensing using multi-core fiber optic cable and parametric curve solutions, Optics express, 2012, 20, 2967–2973.

[4] William L. Ko, W. L. Richards and t. van Tran, Displacement theories for in-flight deformed shape predictions of aerospace structures, NASA Technical Reports 214612, Hampton, Virginia, 2007.

[5] G. C. Foss and E. D. Haugse, Using modal test results to develop strain to displacement transformations, Proceedings of the 13th International Modal Analysis Conference, 1995, 2460, 112.

[6] Zhang H, Zhu X, Gao Z, et al. Fiber Bragg grating plate structure shape reconstruction algorithm based on orthogonal curve net. Journal of Intelligent Material Systems and Structures, 2016, 27(17): 2416-2425.

[7] Alexander Tessler and Jan L. Spangler, A least-squares variational method for full-field reconstruction of elastic deformations in shear-deformable plates and shells, Computer methods in applied mechanics and engineering, 2005, 194, 327–339.

[8] Kefal, I. E. Tabrizi, M. Tansan, E. Kisa and M. Yildiz, An experimental implementation of inverse finite element method for real-time shape and strain sensing of composite and sandwich structures, Composite Structures, 2021, 258, 113431.